Response of coupled noisy excitable systems to weak stimulation

Seiji Tanabe, Tetsuya Shimokawa, Shunsuke Sato, and K. Pakdaman
Department of System and Human Science, Graduate School of Engineering Science, Osaka University, Toyonaka 560-8531 Osaka Japan

(Received 16 February 1999)

It is known that coupling can enhance the response of noisy bistable devices to weak periodic modulation. This work examines whether a similar phenomenon occurs in the active rotator model for excitable systems. We study the dynamics of assemblies of weakly periodically modulated active rotators. The addition of noise to these brings about a number of behaviors that have no counterpart in networks of bistable systems. The analysis of the dynamics of the solution of the Fokker-Planck equation of active rotator networks shows that these new behaviors are similar to generic responses of periodically forced *autonomous* oscillators. This is because noise alone, in the absence of other inputs, can regularize the dynamics of single active rotators through coherence resonance, and lead to regular synchronous activity at the level of networks. We argue that similar phenomena take place in a broad class of excitable systems. [S1063-651X(99)14408-8]

PACS number(s): 87.10.+e, 07.05.Mh

Stochastic resonance (SR) refers to a wide class of phenomena in which the addition of some noise to a nonlinear system enhances the transmission or the detection of a weak signal [1]. For a particle in a double-well potential, the addition of suitable noise to a weak stimulus can maximize measures of the regularity of the interwell hopping. Similar phenomena have been reported in a wide class of systems (for reviews on SR, see [1]). Of special interest has been the possible functional implication of SR-like phenomena in the sensory system [2]. Experimental and theoretical studies have shown that sensory neurons can display SR-like behavior when stimulated by weak signals and noise [3–5].

One method to further enhance SR has been to couple ''resonators.'' Indeed, interactions between the units can favor the cooperative effect of noise over the degradation due to fluctuations. In this way, appropriate coupling can effectively enhance the response of networks and arrays of resonators beyond that of the individual units [6–8]. The fact that nervous systems are composed of large numbers of interacting units susceptible to displaying SR-like behavior suggests that a similar phenomenon may take place in neuronal assemblies. It has been shown that when neurons operate as bistable units, coupling can enhance the response of the network [9]. However, in many instances, neurons act as excitable systems, so that the effect of coupling on their response needs to be studied on its own. This work shows that weakly forced assemblies composed of interacting noisy excitable systems can display richer dynamics than their bistable counterparts. Our emphasis here is on the different qualitatively distinct regimes that such assemblies display rather than measures of the input-output relation, and the influence of a specific parameter on them. These latter issues will be dealt with separately.

We have considered assemblies constituted by FitzHugh-Nagumo, Hodgkin-Huxley, and Morris-Lecar models. All have yielded similar results. In the present paper, we illustrate these by the active rotator (AR) model. Indeed, we have found that, in agreement with [4], this model captures well the essential aspects of the dynamics of the other models, while providing the possibility to understand the underlying mechanisms. An assembly of interacting ARs (referred to as AR network) is described by [10]

$$\frac{d\varphi_i}{dt}=1-a\sin(\varphi_i)+\frac{G}{N}\sum_{j=1}^{N}\sin(\varphi_j-\varphi_i)+A\sin(\Omega t)+\sigma\xi_i, \tag{1}$$

where φ_i evolves on the unit circle [4], $a>1$, $G\geqslant 0$ is the coupling strength, σ is the noise intensity, and ξ_i is white Gaussian noise satisfying $E[\xi_i(t)]=0$ and $E[\xi_i(t)\xi_j(s)]=\delta(t-s)\delta(i-j)$. For $A=0$ and $\sigma=0$, all units stabilize at the unique stable point $\Phi_s=(\varphi_1^s,\ldots,\varphi_n^s)$, with $\varphi_i^s=\arcsin(1/a)$. The system also displays an unstable equilibrium point at $\Phi_u=(\varphi_1^u,\ldots,\varphi_n^u)$, with $\varphi_i^u=\pi-\arcsin(1/a)$, which acts as the firing threshold. A single AR discharges when the trajectory goes over the unstable point and returns to Φ_s along the longer arc.

We consider only *subthreshold* modulations; that is, those that do not elicit a discharge from the single noiseless AR. In the absence of noise, weak subthreshold modulation evokes a synchronous periodic motion around Φ_s. In this regime, units do not rotate around the circle.

The addition of noise to weakly forced AR networks enables some units to cross over the unstable point and make a full rotation around the circle. The dynamics of AR networks in the two extremes of low and large noise levels resembles that of mean-field coupled bistable units [7]. At low noise intensities, the discharges are sporadic, and there is no marked correlation between the firings of individual units besides the one induced by the common input. At large noise levels, units fire frequently, almost independently from one another, leading to an incoherent global discharge rate, which displays oscillations because, even at large noise intensities, units are more likely to fire when the input approaches its maximum value. It is in the transition between these two extreme regimes that AR networks present a wealth of new behavior not present in networks of mean-field coupled bistable devices. These intermediate noise regimes are characterized by two aspects: (a) synchronous firing; that is, coherent activity at the level of the assembly for a broad range of noise intensities, and (b) the patterns of the synchronous discharges, which vary depending on the noise level, with qualitatively distinct patterns corresponding to different noise ranges. In the following paragraph we present a typical scenario of the changes in the global discharge pattern of weakly forced AR networks as the noise is progressively increased in the intermediate range separating the low and large noise regimes.

Once the noise is increased beyond the ‘‘silent’’ regime, sporadic *synchronous* discharges appear. The upper left panel in Fig. 1 shows one example of such firing. As in all other panels in the left-hand column of this figure, it represents the time evolution of the global discharge rate of the network, computed as the proportion of units that fired within a short time window (here 0.1 ms). Thus, the high and narrow peaks in the upper left panel indicate that units fire synchronously, while the variable interdischarge intervals show that these discharges occur irregularly, sometimes skipping one or several input cycles.

Interestingly, further increase in the noise reduces the irregularity of the inter (synchronous) discharge intervals. The global activity then resembles noisy synchronous one-to-one locking, as discharges occur once every cycle and near a preferential phase (left-hand column, second panel in Fig. 1). Further increase in the noise leads to global oscillations with markedly different patterns, which can be easily distinguished one from another.

The four lower panels in the left-hand column of Fig. 1 show examples of such global discharges for four distinct noise levels. The noise intensity increases from top to bottom. The lower three panels are reminiscent of noisy periodic lockings with different locking ratios, while the third panel from the top is more irregular. One remarkable fact is that these patterns are stationary in time, and independent simulations carried with the same parameters always yield the same form of discharge. Furthermore, each of them corresponds to a determined range of noise.

Increasing the noise intensity beyond that of the lowest panel brings no further change in the discharge pattern. Only the amplitude of the oscillations progressively decreases. This is the regime of high noise intensities, when units fire incoherently, yet, on average more frequently at some input phases than others.

The different behavior of the network and the noise-induced transitions between them can be understood through the analysis of the Fokker-Planck equation (FPE) obtained at the limit of large networks [10],

$$\frac{\partial n}{\partial t}(\varphi,t) = -\frac{\partial}{\partial \varphi}[F(\varphi,n(.,t),t)n(\varphi,t)] + D\,\frac{\partial^2 n}{\partial \varphi^2}(\varphi,t), \tag{2}$$

where $n(\varphi,t)d\varphi$ represents the proportion of units within $(\varphi,\varphi+d\varphi)$ at time t, $D=\sigma^2/2$, and

$$F[\varphi,n(.,t),t] = 1 - a\sin(\varphi) + A\sin(\Omega t) + G\int_0^{2\pi}\sin(\varphi'-\varphi)n(\varphi',t)d\varphi'.$$

The right-hand column in Fig. 1 shows the flux through $\varphi = 3\pi/2$ for approximate solutions of Eq. (2) obtained by expanding this equation in Fourier series and truncating after the 30th harmonics (controls truncated at larger harmonics yielded similar results). The 60-dimensional approximate FPE obtained in this way is deterministic with the noise intensity appearing as a parameter. The resemblance between the adjacent panels in the columns of Fig. 1 shows that the

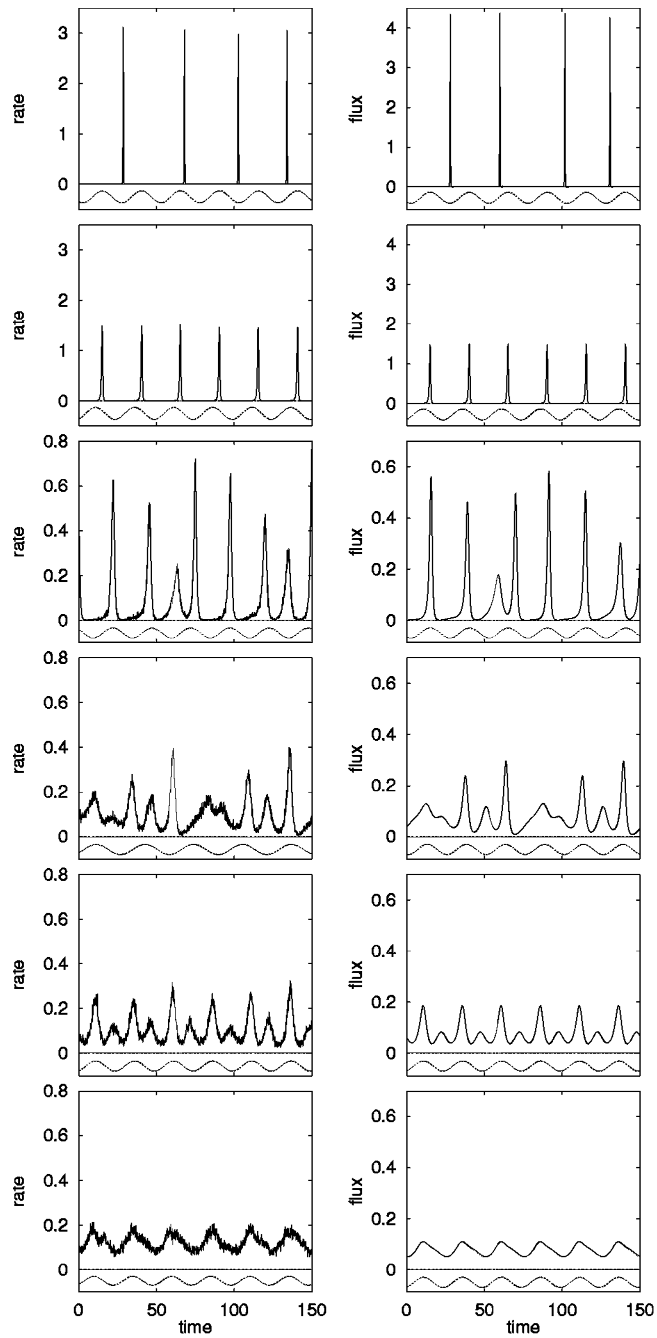

FIG. 1. Left-hand column: global activity of AR networks composed of 10 000 units. Abscissa, time (ms); ordinate, rate (ms^{-1}) defined as the fraction of units crossing $3\pi/2$ from below computed in bins of 0.1 ms. Right-hand column: flux of the solution of the approximate FPE through $3\pi/2$. Abscissa, time (ms); ordinate, flux (ms^{-1}). The ordinate scales have been adjusted for a better view of the patterns. The abscissas represent time after the dissipation of transients. Each panel contains a schematic representation of the sinusoidal input. Parameters: $a=1.01$, $G=1$, $A=0.05$, $\Omega=0.25$, and noise intensity $D=0.02$, 0.08, 0.14, 0.174, 0.2, and 0.3 $(\mathrm{rad}^2/\mathrm{ms})$ from top to bottom.

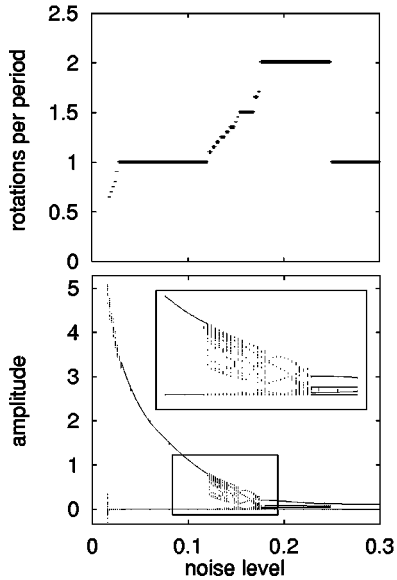

FIG. 2. Noise intensity ($\mathrm{rad}^2/\mathrm{ms}$) vs the average number of synchronous discharges per input cycle (dimensionless) (upper panel), and the local extrema of the flux (ms^{-1}) (lower panel) during a stationary regime of 500 ms duration. Same parameters as in Fig. 1.

approximate FPE captures accurately the dynamics of the simulated networks and its dependence on the noise intensity. The quantitative difference between the firing rate of simulations and the flux of the approximation arises because the latter is instantaneous flow of units across $3\pi/2$, whereas the former is computed over a time-window of width 0.1 ms.

Two conclusions can be drawn from the similarity between the simulations and the solutions of the approximate FPE. (i) Regarding the origin of the variability in the discharge times of the network simulations: in the first and third panels from the top, the irregularities are also present in the solutions of the approximate FPE, thus suggesting that these have a strong nonlinear component. Conversely, in the other panels, the solutions of the approximate FPE are periodic, so that the variability in the corresponding simulations should be mainly attributed to the noise. (ii) The qualitatively distinct regimes observed in the simulations as the noise intensity is varied correspond to different stationary regimes of the approximate FPE, separated by bifurcations. In other words, in this system, the noise intensity acts as a bifurcation parameter, and the dynamics of the solutions change as this parameter crosses critical values.

This offers the possibility to classify the different dynamics according to their characteristics, and determine the range of noise where they occur. This is illustrated in the two panels in Fig. 2. Indeed, the various regimes that appear as the noise is increased can be characterized by two quantities: the average number of synchronous discharges (large amplitude oscillations) per input cycle, and the variations in the amplitude of these oscillations. These two quantities were computed from the solutions of the approximate FPE. The former displays the devil-staircase-like shape typical of forced oscillators (upper panel, Fig. 2). It has plateaus at integers and rational numbers, and increases between such flat segments. The flat segments correspond to periodic solutions locked to the input, while the others yield aperiodic behavior. The changes in the regimes are also apparent at the level of the size of the oscillations (lower panel Fig. 2), where it can be seen that noise intensities beyond the one to one locking range elicit complex responses reminiscent of quasiperiodic and chaotic dynamics (see inset). These diagrams show that the noise intensity acts like a bifurcation parameter, and, as it is increased, the response of AR networks to *subthreshold* stimulation undergoes changes similar to those of either a forced noiseless *autonomous* oscillator, or a noiseless excitable system subject to *suprathreshold* forcing.

The origin of the complex responses of AR networks can be traced to the effect of noise at the level of the single unit. Indeed, a single AR, without periodic forcing, displays three types of dynamics when stimulated by noise. For low noise levels, it fires sporadically and irregularly, while for large noise intensities, it fires abundantly and irregularly. However, there is an intermediate range of noise for which the discharges are more regular [11]. In this regime, ARs operate virtually as *intrinsic* oscillators perturbed by noise. The dynamics of AR networks reflect these three different regimes. For low and large noise intensities, the global discharge is incoherent and sporadic, or incoherent and abundant, respectively. Meanwhile at intermediate noise levels, the AR networks display regular synchronous firing [10,12], as expected in coupled noisy ''pacemaker'' units. In this intermediate regime, the whole network behaves like an intrinsic oscillator. This phenomenon explains the diverse forms of locking and aperiodic patterns that arise in the presence of weak periodic modulation: these are generic responses of forced oscillators. In summary, noise-induced regularity at the level of a single AR is responsible for noise-induced synchronization at the level of the AR networks, which in turn leads to complex dynamics in response to weak periodic modulation.

This mechanism suggests that other networks could also exhibit complex responses when stimulated by weak periodic inputs, as long as they are composed of units susceptible to display some form of noise-induced order. Interestingly, the regularity of the discharge trains of large classes of excitable systems have been shown to be maximal at intermediate noise levels [13]. This phenomenon is known as coherence resonance. Our numerical simulations of networks composed of three neuron models, namely the Hodgkin-Huxley, the FitzHugh-Nagumo, and the Morris-Lecar equations with diffusive as well as pulsatile and synaptic couplings confirm (1) the presence of noise-induced synchronous activity at intermediate noise amplitudes (similar phenomenon have also been analyzed in the spike response neuron model [14]) and (2) for these ranges of noise, the existence of various forms of discharge patterns reminiscent of phase lockings, quasiperiodicity and chaos in response to weak periodic modulation.

Finally, it is important to contrast these results with the dynamics of coupled particles in double-well potentials in order to highlight the novel aspects of the effect of noise on coupled excitable systems. In a forced deterministic bistable system, there is a critical threshold input amplitude $A_c(0)$ beyond which the particle displays interwell motion. For amplitudes below this value, the forced system is bistable because of the coexistence of two stable periodic motions at the bottom of each well. The same remains true for coupled bistable devices. In the case of mean-field coupled bistable devices, without forcing, but in the presence of noise, a similar transition from bistability to monostability takes place as the noise intensity overtakes a critical value D_c [15]. The effect of the addition of weak forcing to the noisy interacting system is to lower the critical noise intensity at which the transition occurs. Similarly, the effect of the addition of noise to the weakly forced system is to lower the critical input amplitude. Thus, when represented in the A-D plane (the noise intensity versus the input amplitude), there is a line, denoted $A_c(D)$, connecting $A_c(0)$ on the y axis to D_c on the x axis, representing the transition from the bistable (subthreshold) regime to the monostable (suprathreshold) regime. For a symmetrical potential, a pitchfork bifurcation takes place along this line [7]. The presence of this line means that the presence of noise lowers the critical threshold input amplitude, so that in effect, increasing the noise intensity leads to interwell jumps. This is the mechanism for the signal enhancement in coupled bistable devices.

A similar scenario can be adapted for the assemblies of AR. In this case, one has to take into account the fact that the forced AR (without noise) displays more complex responses than the bistable device. Indeed, the stroboscopic map associated with the forced AR is a smooth invertible circle map. Thus, when the input amplitude is varied, the forced AR displays diverse phase-locking and quasiperiodic dynamics. Following the same line of reasoning as for the bistable system, one would expect that, in interacting AR assemblies, increasing the noise intensity would bring about changes similar to those that would occur when the input amplitude is increased (in the absence of noise). This scenario would correspond to what is happening in bistable devices. However, our results show that this is not necessarily the case: some of the behaviors that are encountered as the noise is increased cannot occur, no matter what parameters are selected, in the forced coupled deterministic AR. This limitation stems from the fact that families of smooth invertible circle maps can only exhibit phase-locking or quasiperiodicity [16]. They cannot support complex aperiodic responses such as chaos [17], whereas, the inset in the lower panel in Fig. 2 shows that the FPE equation can have such dynamics. In other words, these complex responses are not merely a consequence of the displacement of suprathreshold regimes to lower input amplitudes due to the presence of noise, but constitute new forms of dynamics that arise only when noise is added.

The existence of such noise induced complex responses constitutes a novel aspect of the effect of noise on coupled systems. Indeed, previous studies show that in general noise tends to smear the diverse responses of coupled oscillators into an incoherent overall pattern [18]. Furthermore, this result is relevant in the field of SR because the complex responses represent synchronous discharges; that is, they represent noise-induced amplification of the weak periodic stimulation.

In conclusion, the present results constitute a form of SR that appears in excitable systems, in the form of noise induced complex synchronous discharges, that have no counter part in either bistable systems or the forced deterministic AR assemblies. This appears not only in the patterns of the discharge of the assembly but also in the sequence of noise induced transitions in the dynamics, as the noise intensity is increased. Furthermore, the mechanism underlying this noise effect provides the first evidence of a functionally relevant interplay between coherence resonance and stochastic resonance, and suggests that this interaction can lead to novel forms of SR in neuronal assemblies.

[1] F. Moss, D. Pierson, and D. O'Gorman, Int. J. Bifurcation Chaos Appl. Sci. Eng. **4**, 1383 (1994); A. R. Bulsara and L. Gammaitoni, Phys. Today **49** (3), 39 (1996); L. Gammaitoni *et al.*, Rev. Mod. Phys. **70**, 223 (1998).

[2] R. P. Morse and E. F. Ewans, Nature-Medicine **2**, 928 (1996); P. Cardo *et al.*, Nature (London) **383**, 769 (1996).

[3] J. K. Douglass *et al.*, Nature (London) **365**, 337 (1993); J. E. Levin and J. P. Miller, *ibid.* **380**, 165 (1996); X. Pei and F. Moss, J. Neurophysiol. **76**, 3002 (1996); J. J. Collins, T. T. Imhoff, and P. Grigg, *ibid.* **76**, 642 (1996).

[4] K. Wiesenfeld *et al.*, Phys. Rev. Lett. **72**, 2125 (1994).

[5] A. Longtin, A. R. Bulsara, and F. Moss, Phys. Rev. Lett. **67**, 656 (1991); A. Longtin and D. R. Chialvo, *ibid.* **81**, 4012 (1998); A. Longtin, J. Stat. Phys. **70**, 309 (1993); X. Pei, K. Bachman, and F. Moss, Phys. Lett. A **206**, 61 (1995); A. R. Bulsara *et al.*, Phys. Rev. E **53**, 3958 (1996); T. Shimokawa, K. Pakdaman, and S. Sato, *ibid.* **59**, 3427 (1999); T. Shimokawa *et al.*, *ibid.* **59**, 3461 (1999).

[6] J. F. Lindner *et al.*, Phys. Rev. Lett. **75**, 3 (1995).

[7] P. Jung *et al.*, Phys. Rev. A **46**, 1709 (1992).

[8] M. Morillo, J. Gómez-Ordoñez, and J. M. Casado, Phys. Rev. E **52**, 316 (1995).

[9] A. R. Bulsara and G. Schmera, Phys. Rev. E **47**, 3734 (1993); M. E. Inchiosa and A. R. Bulsara, *ibid.* **52**, 327 (1995).

[10] S. Shinomoto and Y. Kuramoto, Prog. Theor. Phys. **75**, 1105 (1986); H. Sakaguchi, S. Shinomoto, and Y. Kuramoto, *ibid.* **79**, 600 (1988).

[11] D. Sigeti and W. Horsthemke, J. Stat. Phys. **54**, 1217 (1989); W. J. Rappel and S. H. Strogatz, Phys. Rev. E **50**, 3249 (1994); H. Gang *et al.*, Phys. Rev. Lett. **71**, 807 (1993).

[12] C. Kurrer and K. Schulten, Phys. Rev. E **51**, 6213 (1995).

[13] A. Longtin, Phys. Rev. E **55**, 868 (1997); S. G. Lee, A. Nieman, and S. Kim, *ibid.* **57**, 3292 (1998); A. Pikovsky and J. Kurths, Phys. Rev. Lett. **78**, 775 (1997).

[14] J. Pham, K. Pakdaman, and J.-F. Vibert, Phys. Rev. E **58**, 3610 (1998).

[15] M. Shiino, Phys. Rev. A **36**, 2393 (1987).

[16] The stroboscopic map of the periodically forced AR is a smooth invertible circle map regardless of the fact that the AR is excitable ($a>1$) or oscillating ($0<a<1$), or whether the input is sub or suprathreshold.

[17] W. de Melo and S. van Strien, *One Dimensional Dynamics* (Springer-Verlag, Berlin, 1993).

[18] D. Golomb *et al.*, Phys. Rev. A **45**, 3516 (1992).